Bioorganic & Medicinal Chemistry Letters 19 (2009) 2435–2439

Contents lists available at ScienceDirect

Bioorganic & Medicinal Chemistry Letters

journal homepage: www.elsevier.com/locate/bmcl

Significance of interactions of BACE1–Arg235 with its ligands and design of BACE1 inhibitors with P_2 pyridine scaffold

Yoshio Hamada [a], Hiroko Ohta [a], Naoko Miyamoto [a], Diganta Sarma [a], Takashi Hamada [a], Tomoya Nakanishi [a], Moe Yamasaki [a], Abdellah Yamani [a], Shoichi Ishiura [b], Yoshiaki Kiso [a,*]

[a] Department of Medicinal Chemistry, Center for Frontier Research in Medicinal Science and 21st Century COE Program, Kyoto Pharmaceutical University, Yamashina-ku, Kyoto 607-8412, Japan
[b] Department of Life Sciences, Graduate School of Arts and Sciences, University of Tokyo, Meguro-ku, Tokyo 153-8902, Japan

ARTICLE INFO

Article history:
Received 18 February 2009
Accepted 13 March 2009
Available online 18 March 2009

Keywords:
Alzheimer's disease
BACE1
β-Secretase
BACE1 inhibitor

ABSTRACT

Recently, we reported potent substrate-based pentapeptidic BACE1 inhibitors possessing a hydroxymethylcarbonyl isostere as a substrate transition-state mimic. Because these inhibitors contained some natural amino acids, we would need to improve their enzymatic stability in vivo and permeability across the blood–brain barrier, so that they become practically useful. Subsequently, non-peptidic and small-sized BACE1 inhibitors possessing a heterocyclic scaffold, 2,6-pyridenedicarboxylic, chelidamic or chelidonic moiety, at the P_2 position were reported. These inhibitors were designed based on the conformer of docked inhibitor in BACE1. In this study, we discuss the role and significance of interactions between Arg235 of BACE1 and its inhibitor in BACE1 inhibitory mechanism. Moreover, we designed more potent small-sized BACE1 inhibitors with a 2,6-pyridinedicarboxylic scaffold at the P_2 position, that were optimized for the interactions with Arg235 of BACE1.

Amyloid β (Aβ peptide is a main component of senile plaques in the brains of Alzheimer's disease (AD) patients that is involved in AD's pathologies. According to the amyloid hypothesis,[1] β-secretase [BACE1: β-site APP (amyloid precursor protein) cleaving enzyme] appears promising as a molecular target for therapeutic intervention in AD,[2–6] because BACE1 triggers Aβ peptide formation by cleaving APP at the N-terminus of the Aβ domain.[7–12] Previously, we reported potent peptidic BACE1 inhibitors[13–17] ($IC_{50} \sim 1.2$ nM) with a hydroxymethylcarbonyl (HMC) isostere as a substrate transition-state mimic.[18,19] Among them, KMI-429 exhibited effective inhibition of BACE1 activity in cultured cells, and significant reduction of Aβ production in vivo[14b] (by direct administration into the hippocampus of APP transgenic and wild-type mice). Recently, in order to develop practical anti-AD's drug, non-peptidic and small-sized BACE1 inhibitors possessing a 2,6-pyridinedicarboxylic, chelidamic or chelidonic residue at the P_2 position were synthesized on the basis of in-silico design based on the conformer of a virtual inhibitor docked in complex with BACE1 (Fig. 1).[20] However, these non-peptidic compounds exhibited lower BACE1 inhibitory activities than our peptidic KMI-compounds. In this paper, we discussed the role and significance of the interactions between Arg235 of BACE1 and its inhibitors in BACE1 inhibition mechanism. Moreover, we found more potent small-sized BACE1 inhibitors with a 2,6-pyridinedicarboxylic scaffold at the P_2 position that were optimized for interactions with Arg235 of BACE1.

Although we have been considering the role of interaction between Arg235 of BACE1 and its ligands since we started this study, it remained unclear for a long time. The side chain of Arg235 seems to be peculiar, because it is only found outside of the opening of the

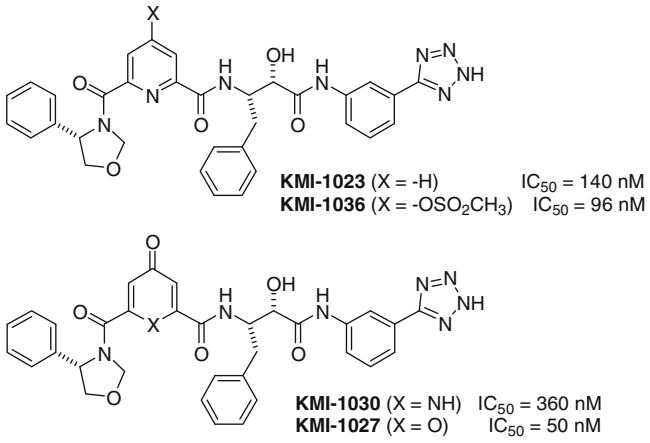

Figure 1. Small-sized BACE1 inhibitors.

* Corresponding author. Tel.: +81 75 595 4635; fax: +81 75 591 9900.
E-mail address: kiso@mb.kyoto-phu.ac.jp (Y. Kiso).

0960-894X/$ - see front matter © 2009 Elsevier Ltd. All rights reserved.
doi:10.1016/j.bmcl.2009.03.049

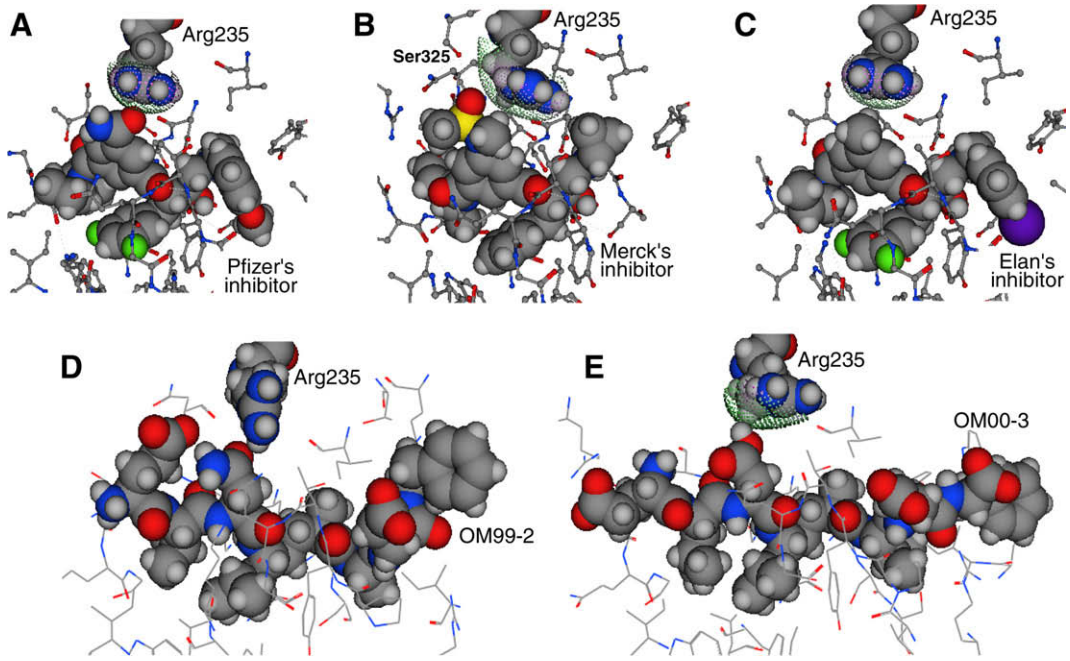

Figure 2. Interactions of BACE1–Arg235 with BACE1 inhibitors in X-ray crystal structures. Space-filling models represent BACE1 inhibitors and BACE1-Arg235. (A) PDB ID:2P83. (B) PDB ID:2B8L. (C) PDB ID:2IQG. (D) PDB ID:1FKN. (E) PDB ID:1M4H.

active site formed by the flap domain of BACE1. Considering that most other amino acid side-chains of BACE1, which can interact with inhibitors or substrates, are found inside the active site between the flap domain and cleft region of BACE1, Arg235 may play an important role in the inhibitory mechanism by inhibitors or in the catalytic action on substrates. Kortum et al.[21] suggested that the amide carbonyl group at the P_2 position of their compound (Pfizer's inhibitor) interacted by O-π stacking with Arg235 of BACE1 from its X-ray crystal structure (PDB ID: 2P83) as shown in Figure 2A. The Arg235 found in BACE1–Merck's inhibitor complex (PDB ID:2B8L) showed a similar figure. Arg235 is 2.8 Å from the *N*-methyl group at the P_2 position of the inhibitor, suggesting that they may interact by CH-π stacking as shown in Figure 2B. The Arg235 in BACE1–Elan's inhibitor complex (PDB ID:2IGQ) also assumed a similar pose as shown in Figure 2C. We compared the publicly-available X-ray crystal structures of BACE1–inhibitor complexes to understand the role of the interactions between BACE1–Arg235 and the P_2 moieties of inhibitors and found a surprising fact that the guanidino group of Arg235 in these crystal structures showed the similar figures flopping over the P_2 region of the inhibitors. Moreover, the nearest distances between the guanidino-plane of Arg235 and the P_2 region showed similar values of about 3 Å, in the X-ray crystal structures of most BACE1–inhibitor complexes (Table 1). However, the Arg235 of the BACE1–OM99-2 complex (PDB ID:IFKN) assumed an exceptionally different pose from most crystal structures of BACE1 complexes (Fig. 2D). The side chain of this Arg235 seemed to be repelled by the P_2 asparagine residue of OM99-2, because this P_2 region interacted with the P_4 glutamic residue by intramolecular hydrogen bonding and cannot interact with Arg235 by stacking. OM00-3 is an inhibitor that is structurally similar to OM99-2. However, the Arg235 in a BACE1 complex (PDB ID:1M4H) with OM00-3 assumed a pose that is similar to Pfizer's, Merck's and Elan's inhibitors, and not to OM99-2, because OM00-3 had no intramolecular hydrogen bond such as OM99-2 as shown in Figure 2E.

From the fact that the guanidino plane of Arg235 in the crystal structures of most BACE1 complexes show similar distances from the P_2 region of the inhibitors regardless of their variety and sizes, we hypothesized an important key point for considering the role of interactions with Arg235: the side chain of Arg235 moves in concert with the inhibitor's size as shown in Figure 3. The guanidino plane of Arg235 pushes down on the P_2 region of the inhibitors, causing them to be affixed in the active site of BACE1. We speculated that a slightly attractive force such as stacking interactions, which cannot be accurately estimated by common molecular mechanics calculations and molecular design programs, played a significant role for packing down the inhibitors effectively in the active site of BACE1. Careful attention should be paid to such weak quantum effects, because softwares tend to calculate all atoms as rigid bodies. Although strong interactions such as hydrogen bonding might activate the apparent enzyme-catalysis for its substrate by improving the 'turn-over' of the enzyme, such strong attractive forces is unfavorable for the action of inhibitors. In fact, our KMI-compounds with hydrogen-bond acceptor or donor, such as asparagine, at the P_2 position showed low inhibitory activities.[5] The fact that our KMI-compounds with an asparagine residue, in which a Swedish mutant APP possessing a high affinity for BACE1 was coded at the same P_2 position, showed disappointing results, seems to support our hypothesis.

The superimposed views of some crystal structures around the active site of BACE1 are shown in Figure 3A and B. The side chain of BACE1's Arg235 has a restricted range of motion. The surface of the β sheet structure that consists of four peptide strands behind BACE1-Arg235 is depicted in Figure 3C, suggesting that the side chain of BACE1-Arg235 slides sideway, not up and down, along the wall of this β-sheet structure. We hypothesized that weak interactions such as stacking halted the sideway motions of BACE1-Arg235, thereby fixing the BACE1-Arg235 above the P_2 region of the inhibitor.

We speculated that an electron-rich halogen atom could interact with the electron-poor guanidino-π orbital by Coulomb's force. If these interactions also involve charge transfer interactions (CT) with directing effects, it is expected that the effects are similar to stacking interactions with directing effects. Hence, we envisioned the BACE1 inhibitors with a halogen atom at the P_2 position.

Table 1
The distances of BACE1–Arg235 from the P_2 parts of inhibitors

PDB ID	The distance (Å) from P_2 part				The closest P_2 atom to guanidino-plane
	N^a	N^b	N^c	Plane[*1]	
2P83	3.2	2.9	2.9	2.7	=O ($CONH_2$)[*2]
2B8L	4.6 (3.7)	4.6 (3.7)	3.9 (2.8)	(2.8)	*N*-Methyl[*3]
2P8H	4.8 (3.8)	4.7 (3.7)	4.1 (2.8)	(3.0)	*N*-Methyl[*3]
2PH6	4.7 (3.8)	4.4 (3.4)	3.9 (2.8)	(2.8)	*N*-Methyl[*3]
20AH	4.1 (3.1)	4.2 (3.4)	3.5 (2.9)	(2.8)	*N*-Methyl[*3]
2QZL	4.5 (3.6)	4.5 (3.7)	3.7 (2.8)	(2.8)	*N*-Methyl[*3]
2P4J	4.4 (4.0)	3.6 (3.3)	3.5 (2.9)	(2.7)	*N*-Methyl[*3]
2IRZ	4.8 (3.9)	4.5 (3.5)	4.0 (2.9)	(2.9)	*N*-Methyl[*3]
2IS0	4.8 (3.9)	4.5 (3.5)	3.9 (2.8)	(2.8)	*N*-Methyl[*3]
2QK5	4.8 (3.9)	4.5 (3.7)	4.1 (3.0)	(3.0)	*N*-Methyl[*3]
2B8V	4.3 (3.4)	4.6 (3.6)	3.8 (2.7)	(2.9)	*N*-Methyl[*3]
1M4H	4.3 (4.1)	5.1 (3.4)	3.9 (3.2)	(2.9)	–COOH (OM00-3)
2HM1	2.7	2.7	2.9	2.4	Pyridine ring
1TQF	4.8	4.8	3.3	2.7	=O($C_6H_5CH_2SO_2$)
1YM2	4.2	3.9	3.5	3.5	–S–(methionine)
2G94	4.3	3.4	4.3	3.3	=O($CH_3SO_2CH_2$–)
2HIZ	2.9	2.6	3.1	2.5	Methylene proton[*4]
1XS7	3.8	3.1	2.6	2.6	Carbonyl (amide)
2IQG	4.4 (3.6)	3.9 (3.2)	4.1 (2.8)	(3.0)	Methyl[*5]
2QK5	4.8 (3.8)	4.5 (3.6)	4.1 (3.1)	(3.1)	Methyl[*5]
2QP8	4.2 (3.1)	4.4 (3.6)	3.9 (3.0)	(2.8)	Methyl[*5]
3CIB	4.4 (3.4)	4.5 (3.6)	4.2 (3.1)	(3.0)	Methyl[*5]
3CIC	4.3 (3.3)	4.4 (3.5)	4.0 (3.0)	(2.9)	Methyl[*5]
3CID	4.2 (3.1)	4.4 (3.5)	4.1 (3.0)	(2.9)	Methyl[*5]
2QMD	4.2 (3.2)	4.4 (3.5)	4.0 (3.1)	(2.9)	Methyl[*5]
2QMF	4.2 (3.2)	4.3 (3.4)	3.9 (2.9)	(2.8)	Methyl[*5]
2QMG	4.0 (3.0)	4.1 (3.4)	3.7 (2.8)	(2.7)	Methyl[*5]
1W51	3.21	4.0	4.0	3.2	Isophthalic ring[*6]
2FDP	4.9	3.7	3.9	3.1	Isophthalic ring[*6]
2VIE	4.7	4.0	3.4	3.0	Pyrrolidone ring
2VJ9	4.2	4.5	3.7	3.7	Pyrrolidone ring
2VIZ	4.3	3.7	2.9	2.6	Pyrrolidone ring
2VNM	4.9	4.2	3.6	3.3	Butanesultan ring
2VIJ	4.9	4.3	3.7	3.6	Butanesultan ring
2VNN	5.6 (4.6)	5.1 (3.4)	4.3 (3.4)	(2.7)	*N*-Methyl
2PH8	5.0 (4.1)	4.7 (3.7)	4.2 (3.5)	(3.3)	*N*-Methyl[*3]

The values in parenthesis show the distances of BACE1-Arg235 from the nearest protons at the P_2 position of the inhibitors.
N^a: ζ-Imino nitrogen atom (flap side).
N^b: ζ-Imino nitrogen atom (cleft side).
N^c: δ-Imino nitrogen atom.
*1: The distance to guanidino-plane from the P_2 region of inhibitor.
*2: Pfizer's inhibitor.
*3: *N*-Methyl-*N*-methanesulfonamide group.
*4: Benzyloxycarbonyl group.
*5: 5-Methylisophthalamide.
*6: An isophthalic-ring's proton.

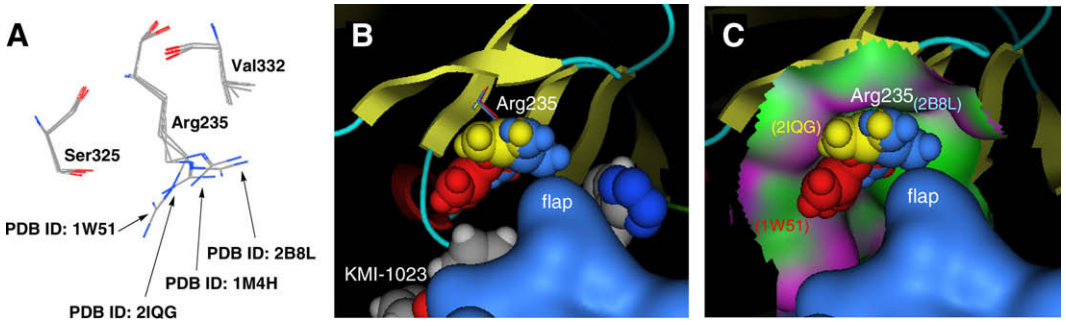

Figure 3. Locations of BACE1–Arg235s in their respective crystal structures. (A) Ser325, Val332 and Arg235 residues from the four crystal structures were superimposed. (B) Superimposed view of three crystal structures around the active site of BACE1. The blue surface model represents the flap domain. The space-filling model behind the flap domain represents BACE1 inhibitor KMI-1023. The blue, yellow and red space-filling models represents the side chain of BACE1–Arg235 in the crystal structures of BACE1, 2B8L, 2IQG and 1W51, respectively. (C) The surface of the β sheet structure behind the BACE1–Arg235 is depicted.

BACE1 inhibitors **1**–**6** were synthesized to connect in tandem with the blocks corresponding to the P_3–P_2 residues and P_1–P_1' residues, respectively, as shown in Scheme 1. Amide bonds were formed by common solution-phase synthesis methods using 1-ethyl-3-(3-dimethylaminopropyl)carbodiimide·HCl (EDC·HCl) in the presence of 1-hydroxybenzotriazole (HOBt) as coupling agents. P_3 residues **9a** and **9b** were synthesized from (*S*)-phenylglycinol and *N*-Boc-4'-fluoro-(*S*)-phenylglycine methyl ester, respectively,

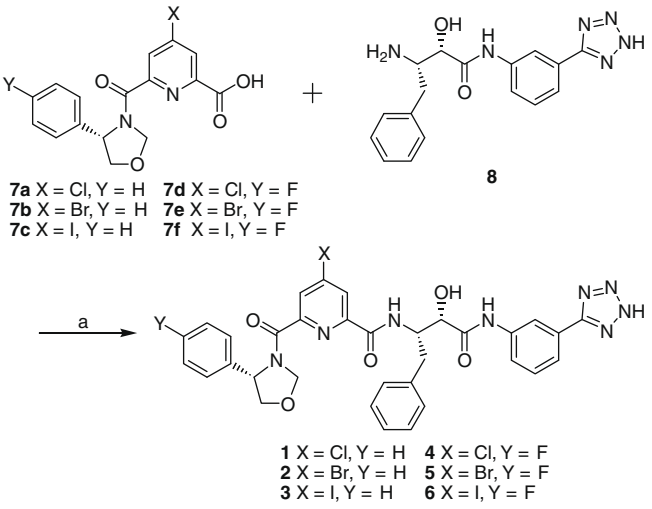

Scheme 1. Reagents: (a) HOBt, EDC·HCl/DMF.

Table 2
BACE1 inhibitory activities

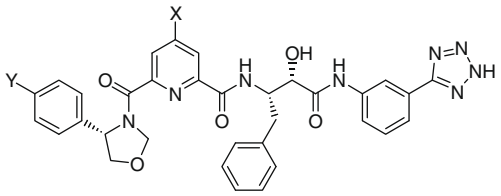

Compound (KMI-No)	X	Y	BACE1 inhibition %		IC_{50} (nM)
			At 2 nM	At 0.2 nM	
KMI-1023	–H	–H	89	62	140
KMI-1036	$-OSO_2CH_3$	–H	96	73	96
1 (KMI-1237)	–Cl	–H	98	87	22
2 (KMI-1256)	–Br	–H	99	88	15
3 (KMI-1293)	–I	–H	99	86	24
4 (KMI-1283)	–Cl	–F	99	91	13
5 (KMI-1303)	–Br	–F	99	93	9
6 (KMI-1302)	–I	–F	99	92	10

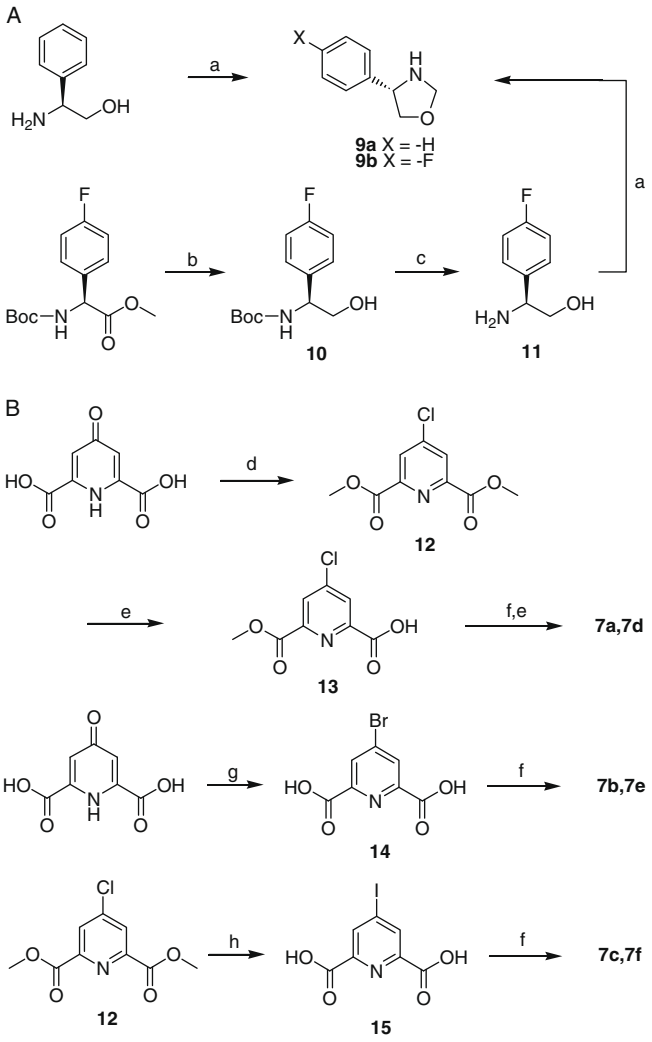

Scheme 2. Reagents and conditions: (a) HCHO, water.;(b) $LiBH_4$/MeOH; (c) 4 N·HCl/dioxane; (d) $SOCl_2$, then MeOH; (e) 1 N NaOH/MeOH; (f) **9a** or **9b**, HOBt, EDC·HCl/DMF; (g) tetra-*n*-butylammonium bromide, P_2O_5, THF, reflux; (h) phosphorous acid, 57% HI aq, 80 °C.

as shown in Scheme 2A, and P_2 residues **13**–**15** with a halogen atom were synthesized from chelidamic acid as shown in Scheme 2B. The P_2 and P_3 residues were coupled to afford P_3–P_2 blocks **7a**–**7f**. The P_1–P_1' block **8** was prepared according to previously reported procedures.[13–17,20] All of the inhibitors were purified by preparative RP–HPLC. BACE1 inhibitory activity of the inhibitors was determined by enzymatic assay using a recombinant human BACE1 and FRET (fluorescence resonance energy transfer) substrate as previously reported.[5]

Synthetic compounds **1**–**3** showed potent BACE1 inhibitory activities as shown in Table 2. From our previous study, introducing a fluorine atom at the P_3 benzene ring of inhibitors improves BACE1 inhibitory activity (data not shown). Hence, we designed BACE1 inhibitors **4**–**6** with a fluorine atom at the P_3 benzene ring. These BACE1 inhibitors exhibited more potent BACE1 inhibitory activities. The fact that an introduction of a halogen atom at the P_2 position in our compounds drastically improved BACE1 inhibitory activity, seems to support our hypothesis.

In conclusion, from the results of our in-silico study using publicly-available crystal structures of BACE1–inhibitor complexes, we proposed a hypothesis concerning the role and significance of the interactions of BACE1–Arg235 with the inhibitors in BACE1 inhibitory mechanism. Next, we designed more potent and small-sized BACE1 inhibitors that were optimized for interactions between the inhibitors and Arg235 of BACE1 based on our hypothesis. Moreover, potent BACE1 inhibitors KMI-1283 (IC_{50} = 13 nM), KMI-1303 (IC_{50} = 9 nM) and KNI-1302 (IC_{50} = 10 nM) were found by introducing a fluorine atom at the P_3 benzene ring. These halogenated inhibitors with higher lipophilicity are expected improved membrane permeability and bioavailability. Thus our study brings us one step closer to developing practical anti-AD's drugs.

Acknowledgements

This study was supported in part by the 'Academic Frontier' Project for Private Universities, matching fund subsidy and the 21st Century COE Program from MEXT (Ministry of Education, Culture, Sports, Science and Technology) of the Japanese Government, and grants from MEXT. We thank Dr. Jeffrey-Tri Nguyen for his help in preparing the manuscript.

References and notes

1. (a) Hong, L.; Koelsch, G.; Lin, X.; Wu, S.; Terzyan, S.; Ghosh, A. K.; Zhang, X. C.; Tang, J. *Science* **2000**, *290*, 150; (b) Sipe, J. D. *Annu. Rev. Biochem.* **1992**, *61*, 947; (c) Selkoe, D. J. *Ann. N.Y. Acad. Sci.* **2000**, *924*, 17; (d) Steiner, H.; Capell, A.;

Leimer, U.; Haass, C. *Eur. Arch. Psychiatric Clin. Neurosci.* **1999**, *249*, 266; (e) Selkoe, D. J. *Ann. Med.* **1989**, *21*, 73.
2. (a) Ghosh, A. K.; Shin, D.; Downs, D.; Koelsch, G.; Lin, X.; Ermolieff, J.; Tang, J. *J. Am. Chem. Soc.* **2000**, *122*, 3522; (b) Ghosh, A. K.; Bilcer, G.; Harwood, C.; Kawahara, R.; Shin, D.; Hussain, K. A.; Hong, L.; Loy, J. A.; Nguyen, C.; Koelsch, G.; Ermolieff, J.; Tang, J. *J. Med. Chem.* **2001**, *44*, 2865.
3. Tung, J. S.; Davis, D. L.; Anderson, J. P.; Walker, D. E.; Mamo, S.; Jewett, N.; Hom, R. K.; Sinha, S.; Thorsett, E. D.; John, V. *J. Med. Chem.* **2002**, *45*, 259.
4. Tamamura, H.; Kato, T.; Otaka, A.; Fujii, N. *Org. Biomol. Chem.* **2003**, *1*, 2468.
5. Shuto, D.; Kasai, S.; Kimura, T.; Liu, P.; Hidaka, K.; Hamada, T.; Shibakawa, S.; Hayashi, Y.; Hattori, C.; Szabo, B.; Ishiura, S.; Kiso, Y. *Bioorg. Med. Chem. Lett.* **2003**, *13*, 4273.
6. (a) Ziora, Z.; Kimura, T.; Kiso, Y. *Drugs Future* **2006**, *31*, 53; (b) Nguyen, J.-T.; Yamani, A.; Kiso, Y. *Curr. Pharm. Des.* **2006**, *12*, 4309.
7. Vassar, R.; Bennett, B. D.; Babu-Khan, S.; Kahn, S.; Mendiaz, E. A.; Denis, P.; Teplow, D. B.; Ross, S.; Amarante, P.; Loeloff, R.; Luo, Y.; Fisher, S.; Fuller, J.; Edenson, S.; Lile, J.; Jarosinski, M. A.; Biere, A. L.; Curran, E.; Burgess, T.; Louis, J. C.; Collins, F.; Treanor, J.; Rogers, G.; Citron, M. *Science* **1999**, *286*, 735.
8. Yan, R.; Bienkowski, M. J.; Shuck, M. E.; Miao, H.; Tory, M. C.; Pauley, A. M.; Brashier, J. R.; Stratman, N. C.; Mathews, W. R.; Buhl, A. E.; Carter, D. B.; Tomasselli, A. G.; Parodi, L. A.; Heinrikson, R. L.; Gurney, M. E. *Nature* **1999**, *402*, 533.
9. Sinha, S.; Anderson, J. P.; Barbour, R.; Basi, G. S.; Caccavello, R.; Davis, D.; Doan, M.; Dovey, H. F.; Frigon, N.; Hong, J.; Jacobson-Croak, K.; Jewett, N.; Keim, P.; Knops, J.; Lieberburg, I.; Power, M.; Tan, H.; Tatsuno, G.; Tung, J.; Schenk, D.; Seubert, P.; Suomensaari, S. M.; Wang, S.; Walker, D.; Zhao, J.; McConlogue, L.; John, V. *Nature* **1999**, *402*, 537.
10. Hussain, I.; Powell, D.; Howlett, D. R.; Tew, D. G.; Meek, T. D.; Chapman, C.; Gloger, I. S.; Murphy, K. E.; Southan, C. D.; Ryan, D. M.; Smith, T. S.; Simmons, D. L.; Walsh, F. S.; Dingwall, C.; Christie, G. *Mol. Cell. Neurosci.* **1999**, *14*, 419.
11. Selkoe, D. J. *Nature* **1999**, *399*, A23.
12. Sinha, S.; Lieberburg, I. *Proc. Natl. Acad. Sci. U.S.A.* **1999**, *96*, 11049.
13. Kimura, T.; Shuto, D.; Kasai, S.; Liu, P.; Hidaka, K.; Hamada, T.; Hayashi, Y.; Hattori, C.; Asai, M.; Kitazume, S.; Saido, T. C.; Ishiura, S.; Kiso, Y. *Bioorg. Med. Chem. Lett.* **2004**, *14*, 1527.
14. (a) Kimura, T.; Shuto, D.; Hamada, Y.; Igawa, N.; Kasai, S.; Liu, P.; Hidaka, K.; Hamada, T.; Hayashi, Y.; Kiso, Y. *Bioorg. Med. Chem. Lett.* **2005**, *15*, 211; (b) Asai, M.; Hattori, C.; Iwata, N.; Saido, T. C.; Sasagawa, N.; Szabó, B.; Hashimoto, Y.; Maruyama, K.; Tanuma, S.; Kiso, Y.; Ishiura, S. *J. Neurochem.* **2006**, *96*, 533.
15. Kimura, T.; Hamada, Y.; Stochaj, M.; Ikari, H.; Nagamine, A.; Abdel-Rahman, H.; Igawa, N.; Hidaka, K.; Nguyen, J.-T.; Saito, K.; Hayashi, Y.; Kiso, Y. *Bioorg. Med. Chem. Lett.* **2006**, *16*, 2380.
16. Hamada, Y.; Igawa, N.; Ikari, H.; Ziora, Z.; Nguyen, J.-T.; Yamani, A.; Hidaka, K.; Kimura, T.; Saito, K.; Hayashi, Y.; Ebina, M.; Ishiura, S.; Kiso, Y. *Bioorg. Med. Chem. Lett.* **2006**, *16*, 4354.
17. Hamada, Y.; Abdel-Rahman, H.; Yamani, A.; Nguyen, J.-T.; Stochaj, M.; Hidaka, K.; Kimura, T.; Hayashi, Y.; Saito, K.; Ishiura, S.; Kiso, Y. *Bioorg. Med. Chem. Lett.* **2008**, *18*, 1649.
18. Mimoto, T.; Imai, J.; Tanaka, S.; Hattori, N.; Takahashi, O.; Kisanuki, S.; Nagano, Y.; Shintani, M.; Hayashi, H.; Akaji, K.; Kiso, Y. *Chem. Pharm. Bull.* **1991**, *39*, 2465.
19. Mimoto, T.; Imai, J.; Tanaka, S.; Hattori, N.; Kisanuki, S.; Akaji, K.; Kiso, Y. *Chem. Pharm. Bull.* **1991**, *39*, 3088.
20. Hamada, Y.; Ohta, H.; Miyamoto, N.; Yamaguchi, R.; Yamani, A.; Hidaka, K.; Kimura, T.; Saito, K.; Hayashi, Y.; Ishiura, S.; Kiso, Y. *Bioorg. Med. Chem. Lett.* **2008**, *18*, 1654.
21. Kortum, S. W.; Benson, T. E.; Bienkowski, M. J.; Emmons, T. L.; Prince, D. B.; Paddock, D. J.; Tomasselli, A. G.; Moon, J. B.; LaBorde, A.; TenBrink, R. E. *Bioorg. Med. Chem. Lett.* **2007**, *17*, 3378.